OsteoArthritis and Cartilage (2006) **14,** 63–70

doi:10.1016/j.joca.2005.08.002

Osteoarthritis and Cartilage

International Cartilage Repair Society

OARSI OSTEOARTHRITIS RESEARCH SOCIETY INTERNATIONAL

3.0 vs 1.5 T MRI in the detection of focal cartilage pathology – ROC analysis in an experimental model

T. M. Link M.D.*, C. A. Sell B.S., J. N. Masi B.A., C. Phan M.D., D. Newitt Ph.D., Y. Lu Ph.D., L. Steinbach M.D. and S. Majumdar Ph.D.

Department of Radiology, University of California, San Francisco, San Francisco, CA, USA

Summary

Objective: To use receiver operator characteristics (ROC) analysis for assessing the diagnostic performance of three cartilage-specific MR sequences at 1.5 and 3 T in detecting cartilage lesions created in porcine knees.

Design: Eighty-four cartilage lesions were created in 27 porcine knee specimens at the patella, the medial and lateral femoral and the medial and lateral tibial cartilage. MR imaging was performed using a fat saturated spoiled gradient echo (SPGR) sequence (in plane spatial resolution/slice thickness: $0.20 \times 0.39\ mm^2$/1.5 mm) and two fat saturated proton density weighted (PDw) sequences (low spatial resolution: $0.31 \times 0.47\ mm^2$/3 mm and high spatial resolution: $0.20 \times 0.26\ mm^2$/2 mm). The images were independently analyzed by three radiologists concerning the absence or presence of lesions using a five-level confidence scale. Significances of the differences for the individual sequences were calculated based on comparisons of areas under ROC curves (A_Z).

Results: The highest A_Z-values for all three radiologists were consistently obtained for the SPGR ($A_Z = 0.84$) and the high-resolution (hr) PDw ($A_Z = 0.79$) sequences at 3 T. The corresponding A_Z-values at 1.5 T were 0.77 and 0.69; the differences between 1.5 and 3 T were statistically significant ($P < 0.05$). A_Z-values for the low-resolution PDw sequence were lower: 0.59 at 3 T and 0.55 at 1.5 T and the differences between 1.5 and 3 T were not significant.

Conclusion: With optimized hr MR sequences diagnostic performance in detecting cartilage lesions was improved at 3 T. For a standard, lower spatial resolution PDw sequence no significant differences, however, were found.

Key words: Cartilage imaging, MRI, High field, ROC-analysis, Experimental study, Focal cartilage pathology.

Introduction

Optimization of cartilage imaging with magnetic resonance imaging (MRI) has evolved in two directions: (1) Quantitative techniques such as dGEMRIC imaging, T1-rho and T2-mapping aim at quantifying the cartilage matrix including glycosaminoglycans and water content as markers of early cartilage degeneration[1–4] and (2) morphologic techniques based on new imaging sequences and higher field strength directly visualize cartilage structure and defects[5–11]. While assessing cartilage biochemistry is important in better understanding degeneration and, potentially, in early treatment of osteoarthritis, morphologic techniques are extremely important in guiding the orthopedic surgeon to better perform cartilage repair such as autologous chondrocyte transplantation and osteochondral autograft transfer[11–18].

Based on promising results in a previous pilot study[19], the purpose of this research project was to assess whether 3 vs 1.5 T provided consistently a better visualization and diagnostic evidence of focal cartilage pathology in fat saturated proton density weighted (PDw) and spoiled gradient echo (SPGR) sequences using receiver operator characteristics (ROC) analysis. A porcine model was used to have optimal control over lesion size, shape and depth. All images were analyzed independently by three radiologists to assess for consistency between different observers.

*Address correspondence and reprint requests to: Thomas M. Link, Department of Radiology, University of California, San Francisco, 400 Parnassus Avenue, A 367, Box 0628, San Francisco, CA 94143-0628, USA. Tel: 1-415-353-8940; Fax: 1-415-476-06161; E-mail: tmlink@radiology.ucsf.edu

Received 15 June 2005; revision accepted 5 August 2005.

Method

PORCINE MODEL AND FOCAL LESION CREATION

The study population consisted of 27 porcine knees that were obtained fresh from a local meat market and frozen for storage at −80 °C. Twenty hours prior to the imaging studies the specimens were thawed to room temperature. A lateral parapatellar approach was used to access the joint space and care was taken to reduce damage of the internal knee structures to a minimum, i.e., the cruciate and collateral ligaments as well as the patellar tendon were preserved. Focal cartilage lesions were created with a ceramic scalpel (Fine Science Tools, San Francisco, CA) to avoid metal artifacts. Cartilage lesions were created analogous to *in vivo* cartilage defects as visualized with arthroscopy and described by McGinty[20] (Fig. 1). In each joint five areas were defined: the patellar surface, the medial and lateral femoral and the medial and lateral tibial joint surfaces. In these 135 joint surfaces, 84 cartilage lesions were created, 81 focal defects and 3 fissure-like defects. Focal lesions were created as (1) full thickness lesions ($n = 39$), (2) lesions with a depth of more than 50% of the total cartilage thickness ($n = 22$) and (3) lesions with a depth of less than 50% of the total cartilage thickness ($n = 23$). Because the lesions

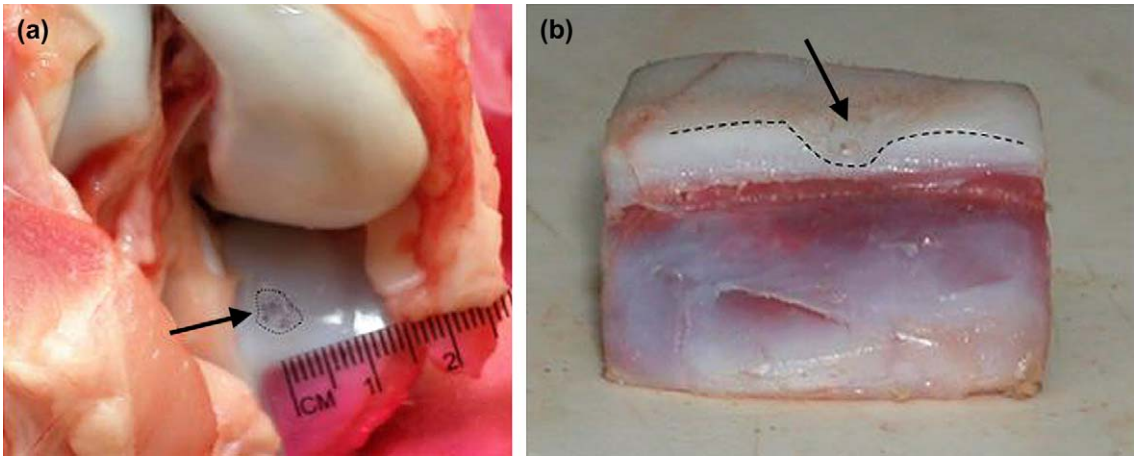

Fig. 1. Specimen photographs showing a full thickness cartilage defect at the medial tibia (a) and a femur section with a more than 50% thickness lesion (b).

varied in shape, the maximum diameter in a sagittal (anteroposterior) orientation was recorded in each case. After lesion creation and measurement, the joints were filled with a mixture of ultrasound gel and water carefully trying to remove remaining air as previously described[19]. In this previous study the signal intensity of the mixture was found to be similar to that of synovial fluid comparing it to clinical studies obtained with similar sequences. The knees were reassembled with special attention to restoring the proper physiological alignment of the articular surfaces and menisci. A transparent latex bag was pulled over the knee from the tibial side and the knee was flexed and extended to remove air from the joint. Finally, the knees were wrapped in parafilm. Care was taken to manually keep the patella in its normal alignment since the lateral retinaculum had been resected during the lesion creation procedure. Each knee was labeled and graphs of each knee were made indicating the exact location, shape, size and depth of the lesions. We also measured the lesions in five of the specimens directly after preparation and after all imaging procedures, when the specimens were dissected, to exclude changes of the lesions' size and depth during storage. But differences in the shape and depth of the lesions were not found.

MR IMAGING

All imaging procedures were performed at 1.5 and 3 T (Signa, GE Medical Systems, Milwaukee, WI, USA) and acquired with two phased array paddle coils (USA Instruments, Aurora, OH, USA for 1.5 T; Nova Medical, Wilmington, MA, USA for 3 T). Both magnetic resonance (MR) systems were equipped with 4 Gauss/cm gradients. Knees were placed in a supine orientation within the center of the coils lined up with the inferior margin of the patella during scanning. Great care was taken to position the specimens in the same way in both scanners. All scans at 1.5 and 3 T were performed immediately, back to back, to prevent changes of specimen condition induced by storage. Three sequences were used at each scanner: a fat saturated PDw standard sequence and fat saturated PDw high-resolution (hr) sequence as well as a hr fat saturated SPGR sequence. The imaging protocols at 1.5 and 3 T are shown in Table I. The low-resolution (lr) PDw sequence was a standard sequence used for imaging at 1.5 T while both hr sequences had been optimized for cartilage imaging at 3 T in a prior study[19]. The rationale to reduce the acquisition time of the SPGR sequence at 3 T was to obtain a clinically applicable SPGR sequence since a major disadvantage

Table I
Imaging sequences at 1.5 and 3 T performed in all specimens (PDw = proton density weighted, lr = low resolution, hr = high resolution, TR = repetition time, TE = echo time, NEX = number of acquisitions, ETL = echo train length, FOV = field of view, BW = band width, ST = slice thickness, Acqu. time = Acquisition time)

	Sequence					
	lr PDw		hr PDw		SPGR	
	Field strength					
	3.0 T	1.5 T	3.0 T	1.5 T	3.0 T	1.5 T
TR (ms)	2000	2000	4000	4000	22	32.9
TE (ms)	35	35	35	35	10	11.5
Flip angle	–	–	–	–	30	30
NEX	2	2	3	3	2	2
ETL	4	4	8	8	–	–
Matrix (pixels)	320 × 224	320 × 224	512 × 384	512 × 384	512 × 256	512 × 256
FOV (cm)	10	10	10	10	10	10
BW (kHz)	15.63	15.63	31.25	31.25	15.63	15.63
ST (mm)	3	3	2	2	1.5	1.5
Acqu. time (min)	3:40	3:48	9:44	9:44	6:33	9:07

of the SPGR sequence is its long acquisition time which makes it more susceptible to motion artifacts.

IMAGE ANALYSIS

All 162 imaging studies (6 sequences obtained from 27 specimens) were reviewed by three radiologists (CP, LS, TML) independently on a PACS workstation (Agfa, Ridgefield Park, NJ, USA). All radiologists were board certified with their experience in musculoskeletal radiology ranging from 6 to 25 years. The radiologists were blinded to lesion location, sequence parameters and field strength. To prevent a learning bias all images were provided to the radiologists in random order and not more than 45 studies per session were reviewed. Time in between reading sessions was at least 96 h. Throughout the reading sessions, ambient light was kept at a minimum, and no time constraints were used.

The radiologists were asked to state whether they were able to detect a lesion in each of the defined knee compartments (medial and lateral tibia and femur as well as patella joint surface). They then assigned one of five levels of confidence (1 = definitely negative, 2 = probably negative, 3 = uncertain, 4 = probably positive, 5 = definitely positive). Location within the compartment had to be stated for each lesion, in case of discordance, if a level of confidence of definitely or probably positive was assigned in an area where no lesion was present it was rated as false positive. Pooled, averaged and individual reader data for a total of 2430 observations (405 per imaging sequence) were analyzed.

The anterior to posterior length of the lesions detected was measured by the individual radiologist and lesion depth was scored using the previously described classification based on the Noyes grading system modified by Recht *et al.*[21] and Noyes and Stabler[22] for MR imaging. In cases where lesions were irregular and displayed different depths, the radiologists were asked to indicate the largest depth. For all measurements and gradings in the imaging studies, the analogue findings during specimen preparation were used as a standard of reference. In addition to better determine the depth of the lesions, specimens were sectioned in the region of the defect after the imaging procedures and cartilage thicknesses in the lesion and the adjacent normal cartilage were measured with a caliper (Fig. 1). Cartilage lesion depth and diameter were measured in consensus by two of the investigators in all specimens (CAS, JNM) to improve accuracy of the measurements.

STATISTICAL ANALYSIS

ROC analyses were performed for each individual sequence at 1.5 and 3 T to estimate their diagnostic performance in detecting cartilage lesions. The location of the lesions as determined during and after specimen preparation was used as a gold standard for ROC analysis. ROC curves were constructed based on five-level ordinal scales assessed by each radiologists using the non-parametric ROC method by DeLong *et al.*[23] with modification according to Zhou and Gatsonis[24]. Areas under the ROC curves (A_Z) were compared between 1.5 and 3 T to estimate the diagnostic performance. A_Z-values were determined for each radiologist, a generalized estimation equation approach for average values was calculated using an S-plus program (Insightful Inc., Seattle, WA) and correlation matrix by Zhou and Gatsonis[24]. Comparing the areas under two or more correlated ROC curves a non-parametric approach[23] was applied. A 0.05 level was used throughout the paper for statistical significance. We also performed kappa statistics to determine the degree of agreement between the three radiologists concerning evaluation of lesion depth.

Results

As shown in Table II, the highest A_Z-values were found at 3 T for the SPGR and the hr PDw sequences, which were significantly higher than the corresponding A_Z-values found at 1.5 T ($P < 0.05$), while for the lr PDw sequence differences between 1.5 and 3 T were not significant ($P > 0.05$). The best performance in detecting cartilage lesions was calculated for the SPGR sequences vs the other sequences both at 1.5 and 3 T. Comparing the A_Z-values for SPGR and hr PDw sequences at 3 and 1.5 T, differences, however, were less pronounced at 3 T, which may be explained by the shorter acquisition time used for the SPGR sequences at 3 T. This also explains the less pronounced increase in diagnostic performance obtained with the SPGR sequence going from 1.5 to 3 T, differences, however, were still significant. Interestingly, A_Z-values for the standard lr PDw sequence were substantially lower both at 1.5 and 3 T and the gain in diagnostic performance at 3 vs 1.5 T was not statistically significant.

Figures 2–4 show representative examples of lesions depicted with the different sequences at 1.5 and 3 T. Differences in image quality are clearly visualized, with higher signal, less noise and better lesion depiction shown at 3 T. More lesions were depicted at 3 T and the confidence in assessing the lesions was increased. Figure 2 shows a lesion at the distal femur as visualized with all three sequences at 3 and 1.5 T. Figures 3 and 4 show lesions that were obtained with PDw and SPGR sequences, respectively, and show better visualization and classification of a lesion at the patella and the tibia. An important finding was also that the increase in diagnostic performance was consistent between the three radiologists (Table II).

Results varied according to the anatomic location (Table III). The highest A_Z-values were found at the femoral joint surfaces, followed by the patella and the tibial joint surfaces. The low A_Z-values at the tibia may be explained by its thin cartilage layer, which makes detection of cartilage defects challenging. The thickest cartilage layer was found at the patella yet A_Z-values were lower than at the femur, but the sagittal orientation used in this study may not be optimal for patellar defects, which are usually better visualized in axial sections.

Table II
ROC analysis for all sequences separately; A_Z-values were obtained from each radiologist and average A_Z-values were calculated

Radiologist	Sequence					
	lr PDw		hr PDw		SPGR	
	Field strength					
	3.0 T	1.5 T	3.0 T	1.5 T	3.0 T	1.5 T
1	0.62	0.56	0.82	0.70	0.81	0.77
2	0.60	0.57	0.88	0.72	0.89	0.80
3	0.59	0.55	0.68	0.65	0.82	0.75
All	0.59	0.55	0.79	0.69	0.84	0.78

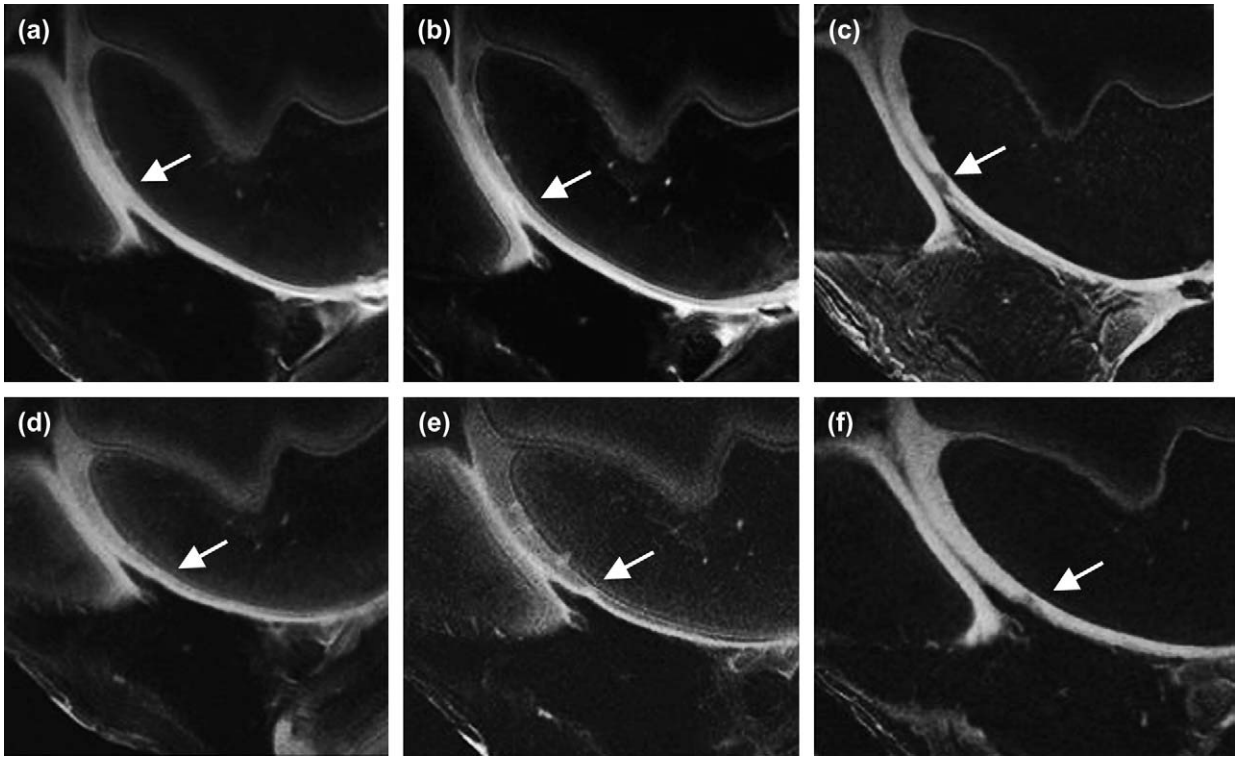

Fig. 2. Sagittal MR images obtained at 3 T (a–c) and 1.5 T (d–f) with all sequences (lr PDw (a,d), hr PDw (b,e) and SPGR (c,f)) demonstrating a grade 2 cartilage lesion, measuring 4 mm at the lateral femoral condyle (arrow). The lesion was not detected in the lr PDw sequences. It was classified as an uncertain lesion in the hr PDw sequence at 1.5 T and as a probable lesion in the 1.5 T SPGR sequence. It was classified as a definite lesion in the corresponding 3 T sequences. Except for the 1.5 T hr IMw the lesion size was correctly measured.

Table IV shows the radiologists's performance in grading lesions. As expected a higher percentage of lesions was correctly graded at 3 vs 1.5 T. The SPGR sequence at 3 T performed best, followed by the hr PDw sequence at 3.0 T, which, however, was only minimally better than the SPGR sequence at 1.5 T. These small differences may be explained by the different slice thicknesses (STs) of the hr PDw and SPGR sequences (2 vs 1.5 mm). Using the lr

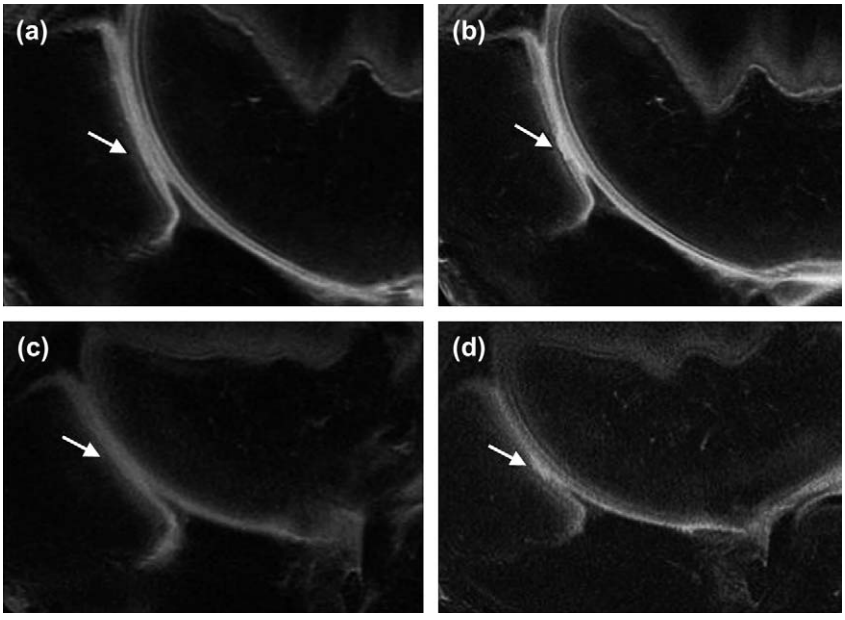

Fig. 3. Sagittal lr (a,c) and hr (b,d) PDw images obtained at 3 T (a,b) and 1.5 T (c,d) demonstrating a grade 3 lesion, 6 mm in diameter at the patella (arrows), that is well visualized in the hr PDw sequence at 3 T (b), but barely visualized in the same sequence at 1.5 T (uncertain lesion) (d). The lesion is not visualized in the lr PDw sequences.

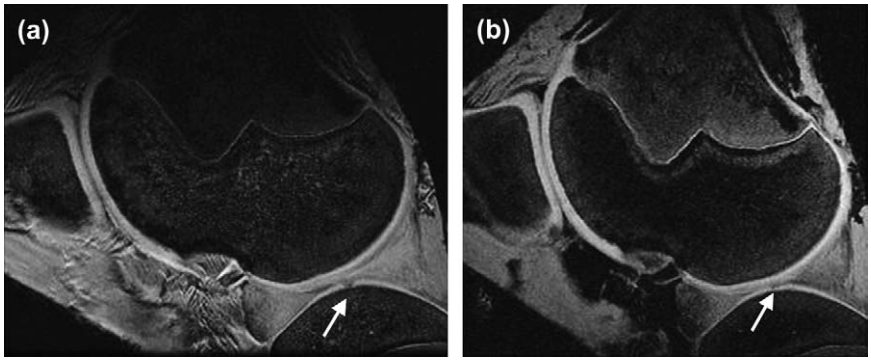

Fig. 4. Sagittal SPGR images obtained at 3 T (a) and 1.5 T (b) showing a grade 3 lesion with a diameter of 4 mm at the tibia. The lesion is well visualized in both sequences but was correctly classified as a grade 3 lesion only at 3 T.

PDw sequences with a ST of 3 mm a substantially lower number of lesions were detected. Please also note that the differences concerning the number of lesions that were correctly graded divided by total number of lesions detected for each sequence were not pronounced and inconsistent between the two field strengths. This, however, may be explained by the additionally detected lesions at 3 T that may have been more difficult to grade, thus reducing overall grading performance. Figure 4 shows a lesion at the tibia that was correctly classified as a grade 3 lesion at 3 T but incorrectly classified as a grade 2 lesion at 1.5 T. Using kappa statistics to assess the agreement in grading between the three radiologists for the different sequences κ-values ranging from 0.25 to 0.58 were found. Agreement was poor in the lr PDw sequences (0.25–0.38) and moderate in the hr sequences (0.42–0.58). It was higher at 3 T than at 1.5 T for the hr sequences (0.58 vs 0.45 for hr PDw sequences and 0.53 vs 0.42 for SPGR sequences).

In Table V, performance in correctly assessing lesion diameter (within a range of ± 1 mm of the diameter measured in the specimens) is presented. As with the grading the best results in assessing the diameter of the lesions in an anteroposterior orientation were determined with the 3 T sequences, meaning that substantially more lesions were correctly measured in the images obtained at 3 T vs in those obtained at 1.5 T. The highest numbers were again detected with the SPGR and hr PDw sequences at 3 T, but the differences between the numbers detected in the 3 T hr PDw and the 1.5 T SPGR sequences were not very pronounced. The highest gain in correctly measured lesions from 1.5 to 3 T was obtained with the lr PDw sequence. Interestingly, the percentage obtained by dividing correctly measured lesions by the total number of detected lesions for each sequence was still higher at 3 vs 1.5 T, consistently for all sequences, which means that even though there were more subtle, additionally visualized lesions, diagnostic performance was better.

Table III
A_Z-values separated for the five different locations at the femur, patella and tibia for all six sequence protocols

A_Z-value	Sequence					
	lr PDw		hr PDw		SPGR	
			Field strength			
	3.0 T	1.5 T	3.0 T	1.5 T	3.0 T	1.5 T
Femur						
Medial	0.73	0.55	0.91	0.71	0.87	0.84
Lateral	0.67	0.66	0.85	0.81	0.93	0.88
Patella	0.51	0.54	0.82	0.74	0.91	0.88
Tibia						
Medial	0.49	0.49	0.79	0.67	0.89	0.65
Lateral	0.54	0.50	0.59	0.53	0.65	0.59

Discussion

The results of this study suggest that 3 T MR imaging may significantly improve the diagnostic performance in assessing focal cartilage lesions compared to 1.5 T MRI. However, dedicated hr sequences may be required to fully exploit the potential of the higher field strength. Results of this ROC analysis also suggest that the increase in diagnostic performance is consistent between different radiologists.

Imaging of articular cartilage is challenging and correct assessment of the cartilage surface and morphology is important to guide therapy. For example, in osteochondritis dissecans drilling procedures may be useful if the cartilage surface above the lesion is intact but not if cartilage defects are shown[25]. In addition cartilage repair procedures such as osteochondral autograft or allograft transfer (mosaicplasty) and autologous chondrocyte implantation require not only exact preoperative planning but also meticulous

Table IV
Number of correctly graded cartilage lesions and total number of detected lesions with absolute numbers for all three radiologists and percentages (correctly graded lesions divided by the total number of lesions) as well as correctly graded lesions divided by the total number of lesions and by the number of detected lesions for the individual sequences

	Sequence					
	lr PDw		hr PDw		SPGR	
			Field strength			
	3.0 T	1.5 T	3.0 T	1.5 T	3.0 T	1.5 T
N_{CG}	38	30	91	76	102	90
N_{CG}/N_T	15%	12%	36%	30%	40%	36%
N_D	70	48	162	129	166	156
N_D/N_T	28%	19%	64%	51%	66%	62%
N_{CG}/N_D	54%	63%	56%	59%	61%	58%

N_{CG} = Number of correctly graded lesions; N_T = Total number of lesions; N_D = Number of detected lesions.

Table V
Measured cartilage lesion size in an antero-posterior orientation in the MR images by each radiologist within a ± 1 mm range compared to size measured in the same orientation in the specimens. Absolute numbers for all three radiologists and relative percentages (divided by the total number of lesions and only the number of detected lesions) for the individual sequences are shown

	Sequence					
	lr PDw		hr PDw		SPGR	
	Field strength					
	3.0 T	1.5 T	3.0 T	1.5 T	3.0 T	1.5 T
N_{MC}	49	23	110	75	121	108
N_{MC}/N_T	19%	9%	44%	30%	48%	43%
N_{MC}/N_D	70%	48%	68%	58%	73%	69%

N_{MC} = Number of correctly measured lesions; N_T = Total number of lesions; N_D = Number of detected lesions.

post-operative follow-up to assess pathology of the repaired cartilage surfaces[11,26–28]. A previous study also stressed the importance of lesions adjacent to the repaired areas, which were visualized with hr imaging and had significant impact on the clinical outcome[29]. Given the requirement of improved cartilage visualization, optimized imaging techniques have been developed[5,8,10,26]. This encompasses new MR sequences with better contrast to noise ratio (CNR) of cartilage and surrounding joint fluid, dedicated coils with better SNR as well as the application of higher field strength.

MR scanners operating at 3 T are increasingly available and, in particular, are attractive since they provide higher signal to noise ratio (SNR) and thus higher spatial resolution without increasing imaging times may be achieved. Technical implications that have to be considered with musculoskeletal 3 T imaging have been previously described[30,31]. Recommended changes at 3 T to improve image quality include shortening of echo time (TE) and increase of repetition time (TR).

A small number of studies have been performed studying the potential of cartilage imaging at 3 T[8,19,32]. In an initial clinical study performed in five volunteers Kornaat *et al.*[8] studied a fat suppressed three-dimensional (3D)-SPGR, a fat suppressed 3D-steady-state free precession (SSFP) and a sagittal Dixon 3D-SSFP sequence at 1.5 and 3 T. All of these sequences yield hyperintense cartilage signal, but signal of the cartilage is lower in the SSFP sequences. While surrounding joint fluid is low or intermediate in signal in the SPGR sequence it is high in the SSFP sequences, which may improve conspicuity of surface lesions. In our study, we also used a fat suppressed (fs) SPGR sequence; the fs PDw sequence we used has similar signal characteristics as the SSFP sequence: in the PDw sequence cartilage is intermediate in signal and synovial fluid is also high in signal intensity. In all of the volunteers, SNR and CNR efficiencies were measured in that previous study and average cartilage thickness measurements were obtained. An expected increase in SNR of 1.6–2.3 was found with 3 T; the increase in SNR was higher in the SSFP sequences than in the SPGR sequence. The measurements of cartilage thickness obtained at 1.5 and 3 T did not show significant differences. Unfortunately since none of the healthy volunteers had cartilage lesions, it was not possible to assess differences in visualization of cartilage pathology in that study.

Fischbach *et al.*[32] examined 12 chondral defects of varying depths, widths, and locations that were created in the retropatellar hyaline cartilage in six sheep cadaver limbs at 1.5 and 3 T. Three fat saturated sequences were studied, a T2-weighted fast spin-echo (FSE) sequence, a two-dimensional (2D) and a 3D gradient-echo (GE) sequences, and ROC analysis was performed. Similar to the results found in our study the 3D GE sequence obtained the highest A_Z-values but differences between 3.0 and 1.5 T were less pronounced than in our study ($A_Z = 0.88$ vs $A_Z = 0.85$). 2D GE imaging was inferior to 3D imaging at both field strengths ($P < 0.05$) but, compared to 1.5 T, lesion detectability was improved at the higher magnetic field of 3.0 T ($A_Z = 0.81$ vs $A_Z = 0.73$). FSE images showed significantly inferior sensitivity and less anatomical detail compared to the GE sequences at both field strengths ($A_Z = 0.64$ vs $A_Z = 0.72$). These results are similar to those found for our lr PDw sequence, yet the A_Z-value was higher for 3.0 T in our study. Limitations of this study include a low number of lesions and specimens, which makes the results of ROC analysis more difficult to comprehend. As in a previous study[8], Fischbach *et al.* also found higher SNR and CNR values for all sequences at 3.0 vs 1.5 T.

In a preliminary study, comparing cartilage imaging at 1.5 and 3 T performed by our group[19], we found a 1.83-fold higher SNR value for a hr PDw sequence and a 1.53-fold increase for an SPGR sequence. However, the SPGR sequence was approximately 25% shorter, and calculating SNR efficiencies and thus adjusting for acquisition time, a 1.76-fold increase of the SPGR sequence at 3 vs 1.5 T was calculated. In the previous study, imaging sequences were optimized in human volunteers and the optimized sequences were used to detect artificially created lesions in 10 porcine specimens. As in our study more sensitive and precise assessment of cartilage lesions was obtained, however, in this previous, preliminary study (1) a substantially smaller number of lesions was analyzed (29 vs 84), (2) only sensitivities in detecting lesions were calculated, (3) no standard sequences were included and (4) images were analyzed by two radiologists in consensus.

Interestingly, our study shows that while optimized hr sequences improve diagnostic performance, a gain of diagnostic information may not be obtained from standard sequences. This also stresses the fact that standard sequences from 1.5 T may not be applied to 3 T with the same parameters but have to be carefully optimized to use their full potential. On the other hand, with optimized sequences imaging times may be reduced while still achieving superior diagnostic performance, as has been shown with the SPGR sequence in this study. This is particularly important for SPGR sequences, which in a clinical setting have a very long acquisition time, making them less feasible for routine protocols.

The use of an experimental model to assess cartilage lesions may be considered as a potential limitation of this study. But ROC analysis requires a true gold standard and lesions should be found in approximately 50% of the analyzed segments. This may be difficult to achieve clinically and for grading of cartilage lesions arthroscopy also may not provide an optimal standard of reference. The fact that we used standard sequences and did not push the limits of spatial resolution in this study may also be considered to be a limitation. However, we feel that optimization of standard sequences at 3 vs 1.5 T is a basic necessity before new sequences should be applied and the limits of spatial resolution should be explored. The use of very similar sequences at 1.5 and 3 T may also be considered as a potential limitation of this study but our aim was to focus the comparison on the different field strengths keeping the

MR parameters similar, yet using sequences optimized for 1.5 T (standard lr IMw sequence) and 3 T (hr IMw and SPGR sequences). For 3 T imaging, in our opinion, the bandwidth (BW) is the key parameter to reduce the more pronounced artifacts. We, therefore, increased the BW to 31.25 in the hr PDw sequence. Increasing the BW for the SPGR sequence, however, did not decrease artifacts but reduced image quality. Increasing the TR to higher numbers was performed for the hr PDw sequence, however, further increase would have made images more T2-weighted, which was not intended. Increasing the echo train length (ETL) does not necessarily reduce imaging time as this also changes the coverage, i.e., by increasing the ETL the coverage may be reduced and thus more slabs may be required to obtain the same coverage, which increases acquisition time substantially. We, therefore, optimized ETL concerning coverage and time.

Future research will have to focus on applying these optimized sequences in a larger clinical population with an arthroscopic standard of reference. In addition, coil development for 3 T imaging is required; preliminary work by Bauer *et al.*[33] has shown that with optimized coil design an up to 3-fold increase in SNR may be obtained with 3 T vs standard 1.5 T imaging. A number of new imaging sequences have been suggested to improve cartilage imaging at 1.5 T[2,6,7,29,33–35] and the application and modification of these sequences to 3 T would also be an aim of future research projects.

Computer aided localization and quantification of focal lesions of cartilage has been approached using a variety of techniques[36,37] and compared with arthroscopic measurements[38]. Although Lee *et al.*[38] demonstrated the feasibility of making measurements at 1.5 and 3 T, and did not show statistically significant results in determining lesion sizes at 1.5 and 3 T, it must be added, the studies were early studies focused at the development of the computerized algorithm and did not optimize the image acquisition and resolutions achievable at 3 T. Further developments of automatic segmentation of cartilage and of algorithms for the quantification of focal lesions utilizing optimized cartilage-specific sequences for 3 T may also represent an important research direction.

In conclusion this study has shown the potential of 3 T MR imaging to increase diagnostic performance in assessing pathology of the cartilage surface using ROC-methodology. It should be considered that cartilage dedicated sequences have to be optimized for imaging at 3 T and applying 1.5 T sequences to 3 T may not provide better results. Future studies are required to validate these findings in a clinical environment.

Acknowledgments

The authors would like to thank Jan Bauer, M.D., for his help with the statistical calculations. Niles Bruce, RT, provided important help with the imaging procedures.

References

1. Burstein D, Bashir A, Gray ML. MRI techniques in early stages of cartilage disease. Invest Radiol 2000;35: 622–38.
2. Burstein D, Gray M. New MRI techniques for imaging cartilage. J Bone Joint Surg Am 2003;85-A(Suppl 2): 70–7.
3. Dunn TC, Lu Y, Jin H, Ries MD, Majumdar S. T2 relaxation time of cartilage at MR imaging: comparison with severity of knee osteoarthritis. Radiology 2004;232: 592–8.
4. Regatte RR, Akella SV, Wheaton AJ, Lech G, Borthakur A, Kneeland JB, *et al*. 3D-T1rho-relaxation mapping of articular cartilage: *in vivo* assessment of early degenerative changes in symptomatic osteoarthritic subjects. Acad Radiol 2004;11:741–9.
5. Gold GE, McCauley TR, Gray ML, Disler DG. What's new in cartilage? Radiographics 2003;23: 1227–42.
6. Gold GE, Fuller SE, Hargreaves BA, Stevens KJ, Beaulieu CF. Driven equilibrium magnetic resonance imaging of articular cartilage: initial clinical experience. J Magn Reson Imaging 2005;21:476–81.
7. Hargreaves BA, Gold GE, Beaulieu CF, Vasanawala SS, Nishimura DG, Pauly JM. Comparison of new sequences for high-resolution cartilage imaging. Magn Reson Med 2003;49:700–9.
8. Kornaat PR, Reeder SB, Koo S, Brittain JH, Yu H, Andriacchi TP, *et al*. MR imaging of articular cartilage at 1.5 T and 3.0 T: comparison of SPGR and SSFP sequences. Osteoarthritis Cartilage 2005;13: 338–44.
9. Link T, Majumdar S, Peterfy C, Daldrup H, Uffmann M, Dowling C, *et al*. High resolution MRI of small joints: impact of spatial resolution on diagnostic performance and SNR. Magn Reson Imaging 1998;16:147–55.
10. Disler DG, Recht MP, McCauley TR. MR imaging of articular cartilage. Skeletal Radiol 2000;29:367–77.
11. Recht M, White LM, Winalski CS, Miniaci A, Minas T, Parker RD. MR imaging of cartilage repair procedures. Skeletal Radiol 2003;32:185–200.
12. Andres BM, Mears SC, Wenz JF. Surgical treatment options for cartilage defects within the knee. Orthop Nurs 2001;20:27–31.
13. Ueblacker P, Burkart A, Imhoff AB. Retrograde cartilage transplantation on the proximal and distal tibia. Arthroscopy 2004;20:73–8.
14. Sanders TG, Mentzer KD, Miller MD, Morrison WB, Campbell SE, Penrod BJ. Autogenous osteochondral "plug" transfer for the treatment of focal chondral defects: postoperative MR appearance with clinical correlation. Skeletal Radiol 2001;30:570–8.
15. Horas U, Pelinkovic D, Herr G, Aigner T, Schnettler R. Autologous chondrocyte implantation and osteochondral cylinder transplantation in cartilage repair of the knee joint. A prospective, comparative trial. J Bone Joint Surg Am 2003;85-A:185–92.
16. Hangody L, Fules P. Autologous osteochondral mosaicplasty for the treatment of full-thickness defects of weight-bearing joints: ten years of experimental and clinical experience. J Bone Joint Surg Am 2003; 85-A(Suppl 2):25–32.
17. Hui JH, Chen F, Thambyah A, Lee EH. Treatment of chondral lesions in advanced osteochondritis dissecans: a comparative study of the efficacy of chondrocytes, mesenchymal stem cells, periosteal graft, and mosaicplasty (osteochondral autograft) in animal models. J Pediatr Orthop 2004;24:427–33.
18. Bentley G, Biant LC, Carrington RW, Akmal M, Goldberg A, Williams AM, *et al*. A prospective, randomised comparison of autologous chondrocyte implantation versus mosaicplasty for osteochondral defects in the knee. J Bone Joint Surg Br 2003;85: 223–30.

19. Masi J, Sell C, Phan C, Han E, Newitt D, Steinbach L, *et al*. Cartilage imaging at 3 Tesla versus 1.5 Tesla – preliminary results in a porcine model. Radiology 2005;236:140–50.
20. McGinty JB. Operative Arthroscopy. New York: Raven Press 1996.
21. Recht M, Piraino D, Paletta G, Schils J, Belhobek G. Accuracy of fat-suppressed three-dimensional spoiled gradient-echo FLASH MR Imaging in the detection of patellofemoral articular cartilage abnormalities. Radiology 1996;198:209–12.
22. Noyes FR, Stabler CL. A system for grading articular cartilage lesions at arthroscopy. Am J Sports Med 1989;17:505–13.
23. DeLong ER, DeLong DM, Clarke-Pearson DL. Comparing the areas under two or more correlated receiver operating characteristic curves: a nonparametric approach. Biometrics 1988;44:837–45.
24. Zhou XH, Gatsonis CA. A simple method for comparing correlated ROC curves using incomplete data. Stat Med 1996;15:1687–93.
25. Kawasaki K, Uchio Y, Adachi N, Iwasa J, Ochi M. Drilling from the intercondylar area for treatment of osteochondritis dissecans of the knee joint. Knee 2003;10:257–63.
26. Verstraete KL, Almqvist F, Verdonk P, Vanderschueren G, Huysse W, Verdonk R, *et al*. Magnetic resonance imaging of cartilage and cartilage repair. Clin Radiol 2004; 59:674–89.
27. Gold GE, Bergman AG, Pauly JM, Lang P, Butts RK, Beaulieu CF, *et al*. Magnetic resonance imaging of knee cartilage repair. Top Magn Reson Imaging 1998;9:377–92.
28. Bohndorf K. Imaging of acute injuries of the articular surfaces (chondral, osteochondral and subchondral fractures). Skeletal Radiol 1999;28:545–60.
29. Woertler K, Settles M, Martinek V, Stollfuss J, Rummeny E. Patellar osteochondral autograft transplantation: assessment with high-resolution MR imaging at 1.5 T. Eur Radiol 2005;15:S1–S211.
30. Gold GE, Han E, Stainsby J, Wright G, Brittain J, Beaulieu C. Musculoskeletal MRI at 3.0 T: relaxation times and image contrast. AJR Am J Roentgenol 2004;183: 343–51.
31. Gold GE, Suh B, Sawyer-Glover A, Beaulieu C. Musculoskeletal MRI at 3.0 T: initial clinical experience. AJR Am J Roentgenol 2004;183:1479–86.
32. Fischbach F, Bruhn H, Unterhauser F, Ricke J, Wieners G, Felix R, *et al*. Magnetic resonance imaging of hyaline cartilage defects at 1.5 T and 3.0 T: comparison of medium T2-weighted fast spin echo, T1-weighted two-dimensional and three-dimensional gradient echo pulse sequences. Acta Radiol 2005;46:67–73.
33. Bauer J, Ross C, Li X, Carballiodo-Gamio J, Banerjee S, Krug R, *et al.* Optimization and reproducibility evaluation of volumetric cartilage measurements of the knee at 1.5 T and 3 T. In: Proceedings of the ISMRM, Miami; 2005.
34. Miller KL, Hargreaves BA, Gold GE, Pauly JM. Steady-state diffusion-weighted imaging of *in vivo* knee cartilage. Magn Reson Med 2004;51:394–8.
35. Regatte RR, Akella SV, Borthakur A, Kneeland JB, Reddy R. *In vivo* proton MR three-dimensional T1rho mapping of human articular cartilage: initial experience. Radiology 2003;229:269–74.
36. McGibbon CA, Trahan CA. Measurement accuracy of focal cartilage defects from MRI and correlation of MRI graded lesions with histology: a preliminary study. Osteoarthritis Cartilage 2003;11:483–93.
37. Lee KY, Dunn TC, Steinbach LS, Ozhinsky E, Ries MD, Majumdar S. Computer-aided quantification of focal cartilage lesions of osteoarthritic knee using MRI. Magn Reson Imaging 2004;22:1105–15.
38. Lee KY, Masi JN, Sell CA, Schier R, Link TM, Steinbach LS, *et al*. Computer-aided quantification of focal cartilage lesions using MRI: accuracy and initial arthroscopic comparison. Osteoarthritis Cartilage 2005;13: 728–37.